

# EFT methods for Binary Inspirals, II

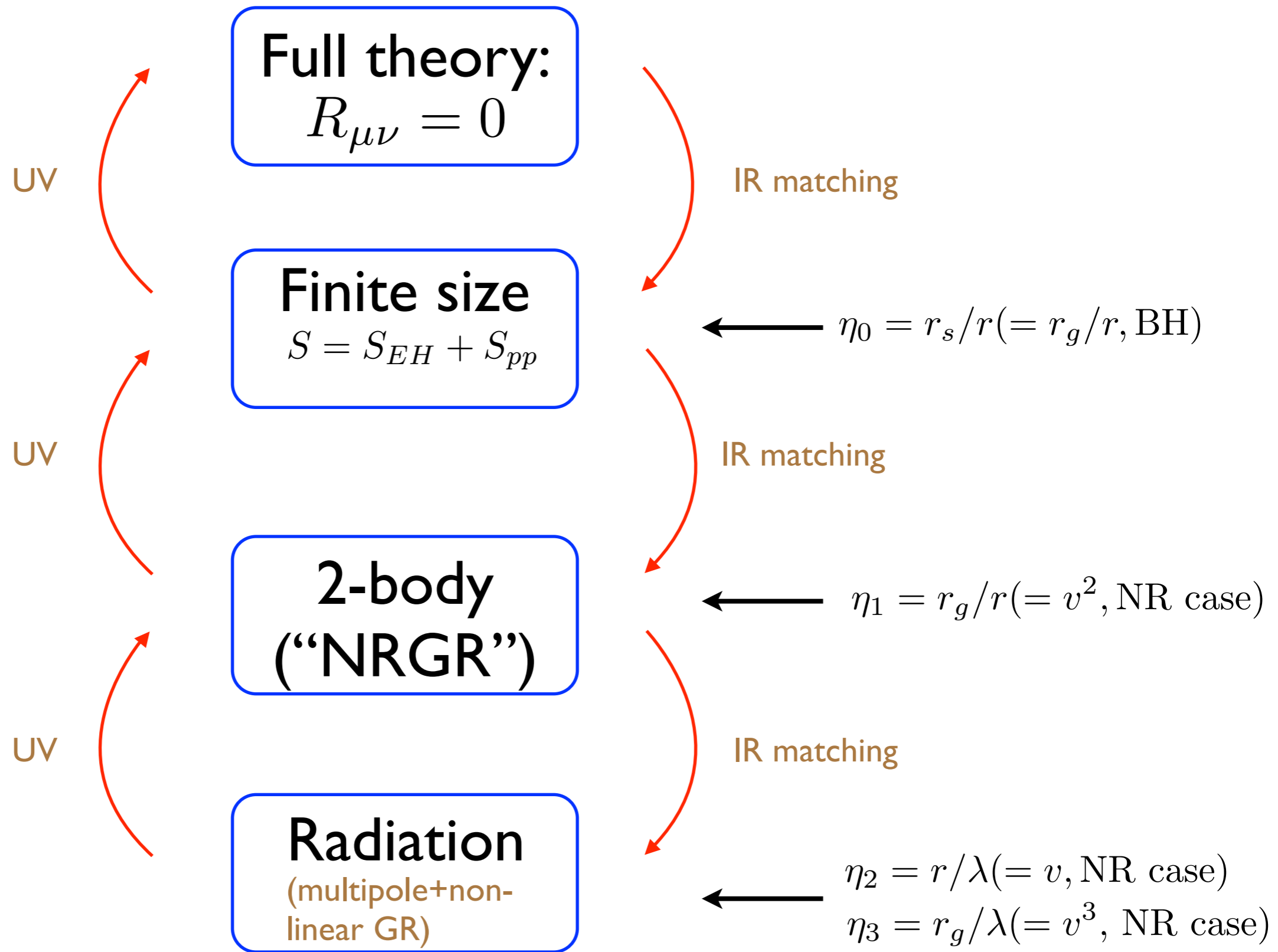
Walter Goldberger  
Yale U.

Based on: W.G., A. Ross, I. Rothstein ; PRD '13

⋮

W.G. + Rothstein, '04.

# Tower of gravity EFTs:



Independent EFTs with distinct expansion parameter coincide in PN limit.  
UV divergence in  $\text{EFT}_{i+1}$  corresponds to IR effect in  $\text{EFT}_i$

# EFT II: 2-body bound state

This is a theory of 2 pt non-relativistic particles, interacting gravitationally and emitting radiation:

$$S = S_{EH} + S_{pp}$$

where now,

$$S_{pp} = - \sum_{a=1,2} \int d\tau_a m_a + \sum_{a=1,2} \int d\tau_a \left( c_a^E E_{\mu\nu}^2 + c_a^B B_{\mu\nu}^2 \right) + \dots$$

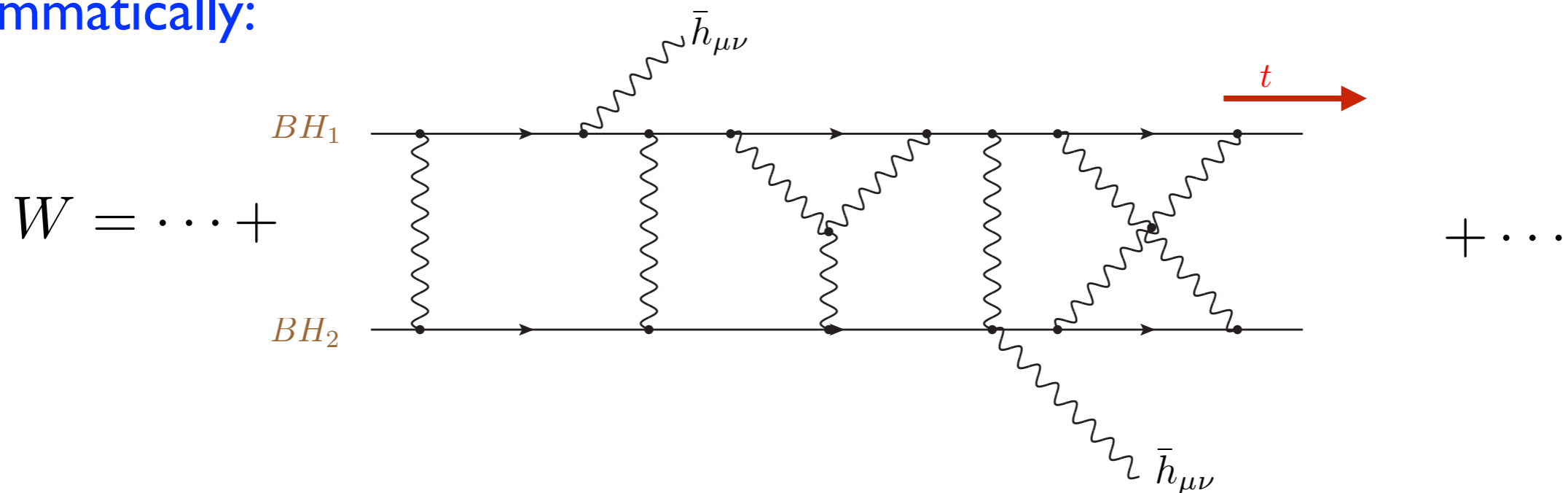
ignoring spin, finite size, etc.

## The gravitational “Wilson line”

$$W = \exp i\Gamma[\bar{h}, x_a] = \int [\mathcal{D}h_{\mu\nu}]_{\text{b.c.'s}} e^{iS[h, \bar{h}, x_a]}$$

generates all the observables of the (classical) binary system.

Diagrammatically:



$$= e^{\Sigma}(\text{BH irreducible diagrams})$$

where we split up the metric into a background field and a “fluctuating part”:

$$g_{\mu\nu} = \eta_{\mu\nu} + \bar{h}_{\mu\nu} + h_{\mu\nu}$$

background

fluctuation

and integrate out fluctuations.

For example,

$$\Gamma[\bar{h} = 0, x_a] = \int dt L(\mathbf{x}_a(t), \dot{\mathbf{x}}_a(t)) = \text{two-body Lagrangian}$$

generates the equations of motion for the BH trajectories

The linear term in the background defines an effective energy-momentum tensor:

$$\Gamma[\bar{h} =, x_a] = \dots + \frac{1}{2m_{Pl}} \int d^4x T^{\mu\nu}(x) \bar{h}_{\mu\nu} + \dots$$

$$\partial_\mu T^{\mu\nu}(x) = 0$$

(Ward id. for diff invariance)

which can be used to compute radiation at infinity

In particular, with standard in/out (Feynman) b.c.'s, graviton emission amplitude is

$$\mathcal{A}_{h=\pm 2}(k) = \int d^4x e^{ik \cdot x} \epsilon_{\mu\nu}^*(h, k) T^{\mu\nu}(x)$$

and the graviton emission rate over  $T \rightarrow \infty$

$$d\Gamma_h(\mathbf{k}) = \frac{1}{T} \frac{d^3\mathbf{k}}{(2\pi)^3 2|\mathbf{k}|} |\mathcal{A}_h(\mathbf{k})|^2,$$

yield time-averaged energy and momentum emission rates:

$$\langle \dot{P}^\mu \rangle_{h=\pm 2} = \int k^\mu d\Gamma_h(\mathbf{k}),$$

$$\langle \dot{\mathbf{J}} \rangle = 2 \int \mathbf{n} d\Gamma_{h=2}(\mathbf{k}) - 2 \int \mathbf{n} d\Gamma_{h=-2}(\mathbf{k}),$$

Using in/in boundary conditions (as in cosmology) gives instantaneous observables, e.g. radiation field at infinity:

$$h_{\mu\nu}(\mathbf{x} \rightarrow \infty, t) = \int d^4y D_{\mu\nu;\alpha\beta}^{\text{ret}}(x - y) T^{\alpha\beta}(y)$$

which yields the time-dep. waveform seen in the detector.

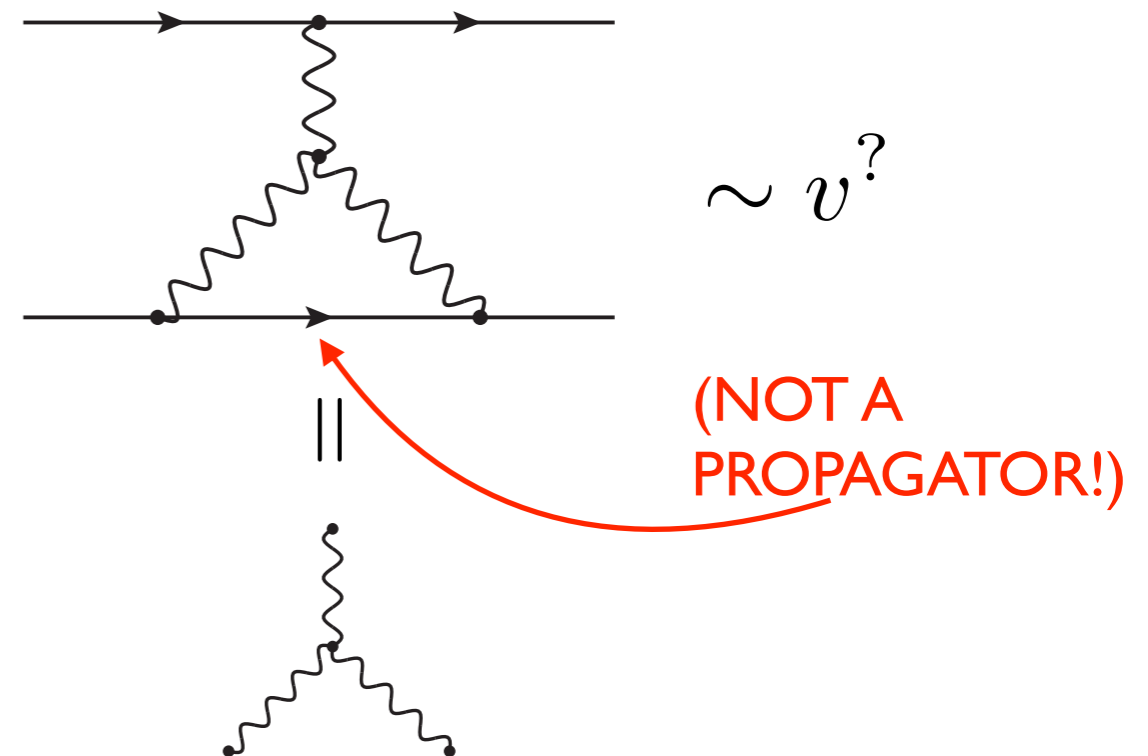
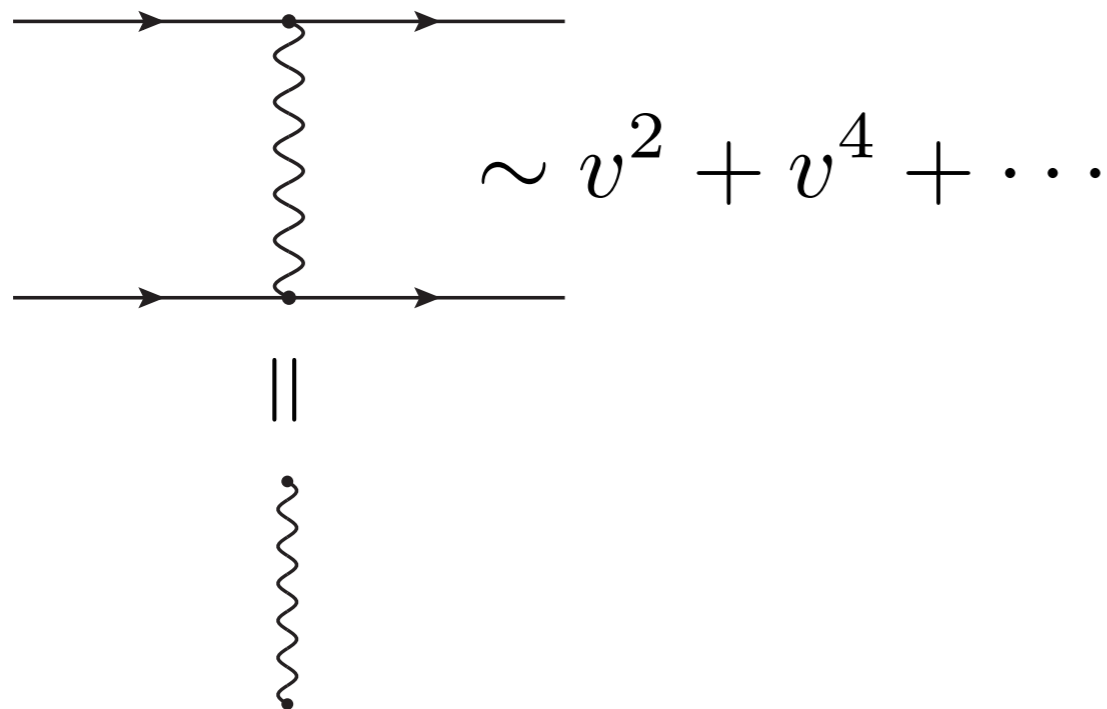
To compute the generating function  $W$  one could use standard covariant Feynman rules obtained by expanding  $S_{EH} = -2m_{Pl}^2 \int d^4x \sqrt{g} R$

$$g_{\mu\nu} = \eta_{\mu\nu} + h_{\mu\nu}/m_{Pl}$$

w/ e.g

$$\mu, \nu \xrightarrow{k} \alpha, \beta = \frac{i}{k^2} P_{\mu\nu; \alpha, \beta} \quad (\text{Feynman gauge})$$

However, these Feynman rules are not optimal for the NR limit  $v \ll 1$ . The diagrams don't have manifest power counting in the exp. parameter:



The problem is that the diagrams involve momentum integrals over all momentum regions. However, for NR kinematics, two momentum space configurations dominate:

“potential”:  $(E \sim 0, \vec{p} \sim 1/r)$  (off-shell)

“radiation”:  $(E \sim v/r, \vec{p} \sim v/r)$

The solution to this problem is well known from NRQED/NRQCD and HQET. Decompose graviton into distinct momentum modes and “pull out” short scales:

$$g_{\mu\nu}(x) = \eta_{\mu\nu} + \bar{h}_{\mu\nu}(x) + \sum_{\mathbf{k}} e^{i\mathbf{k}\cdot\mathbf{x}} H_{\mathbf{k}\mu\nu}(x^0)$$

$\partial_\mu H_{\mathbf{k}} \sim \frac{v}{r} H_{\mathbf{k}}$

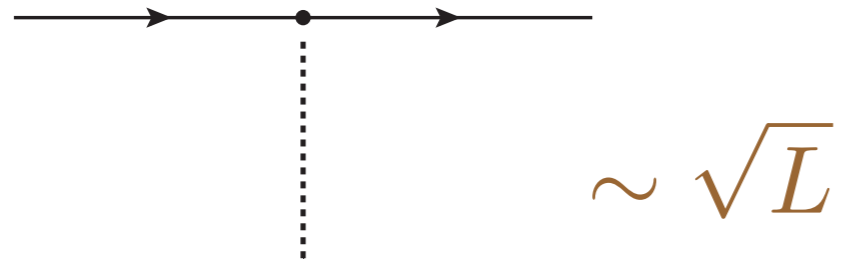
$\partial_\mu \bar{h} \sim \frac{v}{r} \bar{h}$

$\mathbf{k} \sim \frac{1}{r}$

The radiation mode can be regarded as long wavelength background field in which potential gravitons propagate

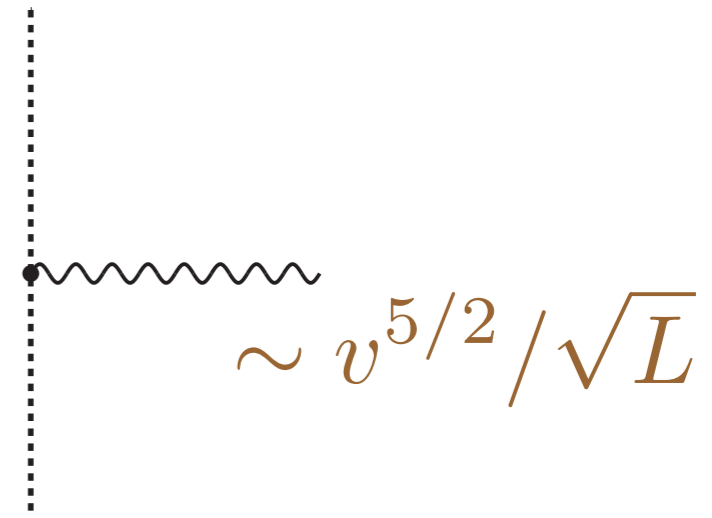


In addition, need to multipole expand the couplings of the radiation mode to the particles and to the potentials. This yields an effective Lagrangian with manifest power counting in velocity:



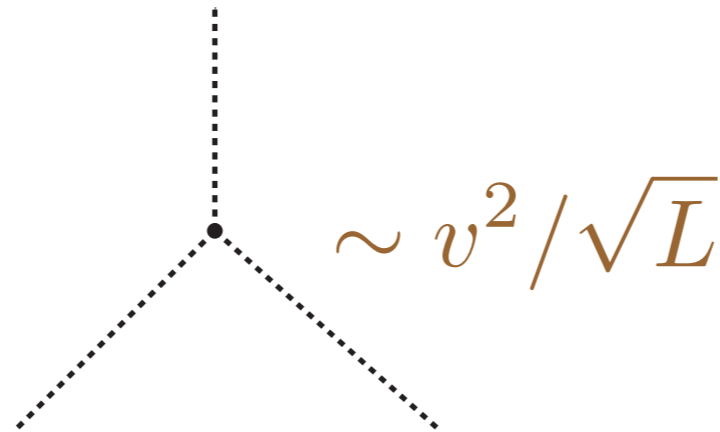
$$\sim \sqrt{L}$$

Pt. particle-Newton  
potential  
interaction:



$$\sim v^{5/2} / \sqrt{L}$$

Radiation-potential  
interaction

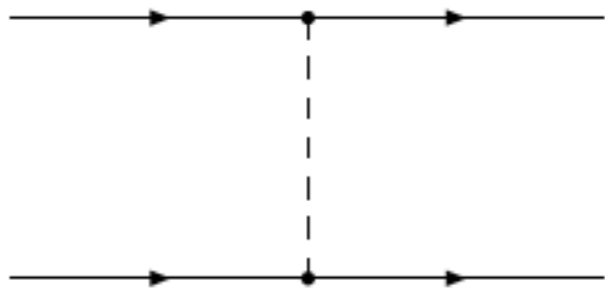


$$\sim v^2 / \sqrt{L}$$

Potential graviton cubic  
self-interaction

By connecting vertices together, generate the 2-body potentials and the interactions of matter with radiation. Drop quantum corrections  $\sim \hbar/L \ll 1$

Leading order:  
Newton  
(1687)

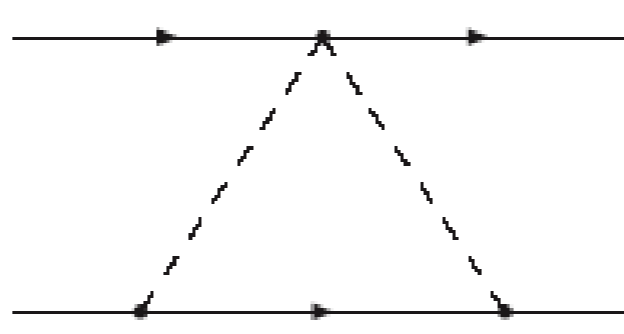
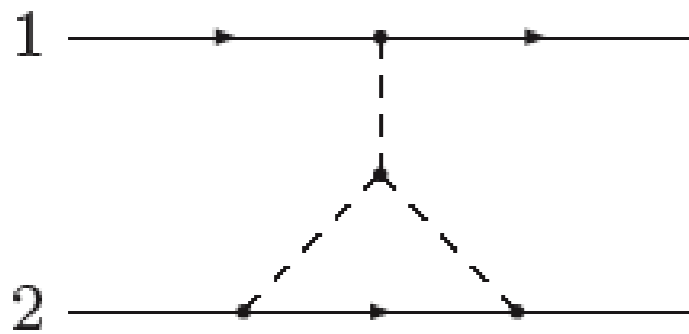
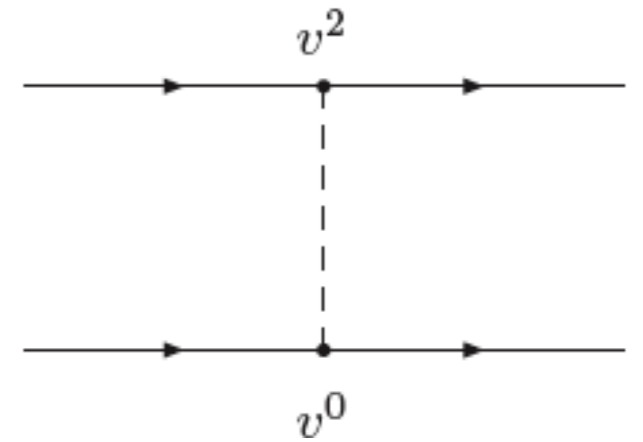
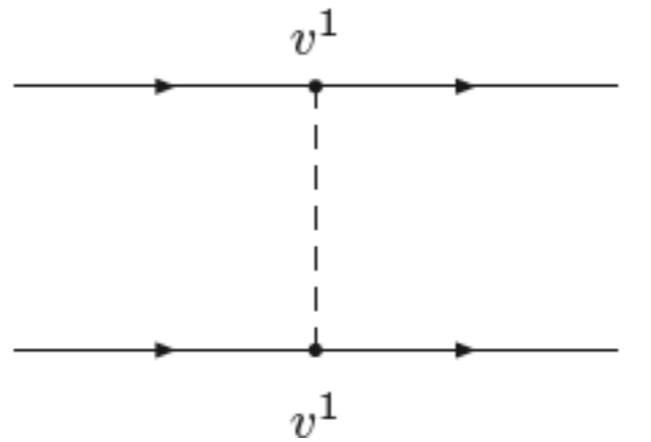
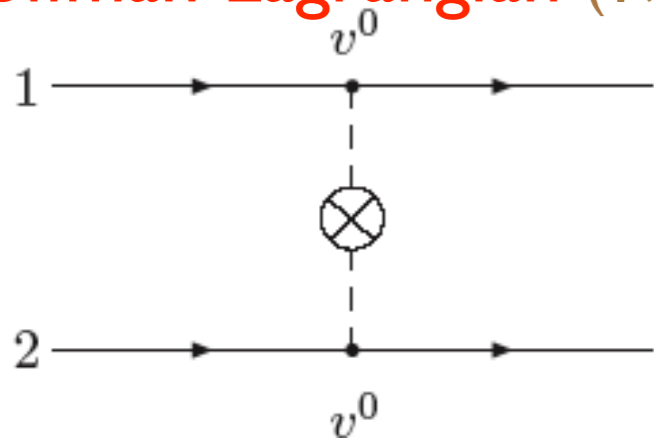


(a)



$$L = \frac{1}{2} \sum_a m_a \vec{v}_a^2 + \frac{G_N m_1 m_2}{r}$$

Next-to-leading (IPN): Einstein-Infeld  
Hoffman Lagrangian (1938)

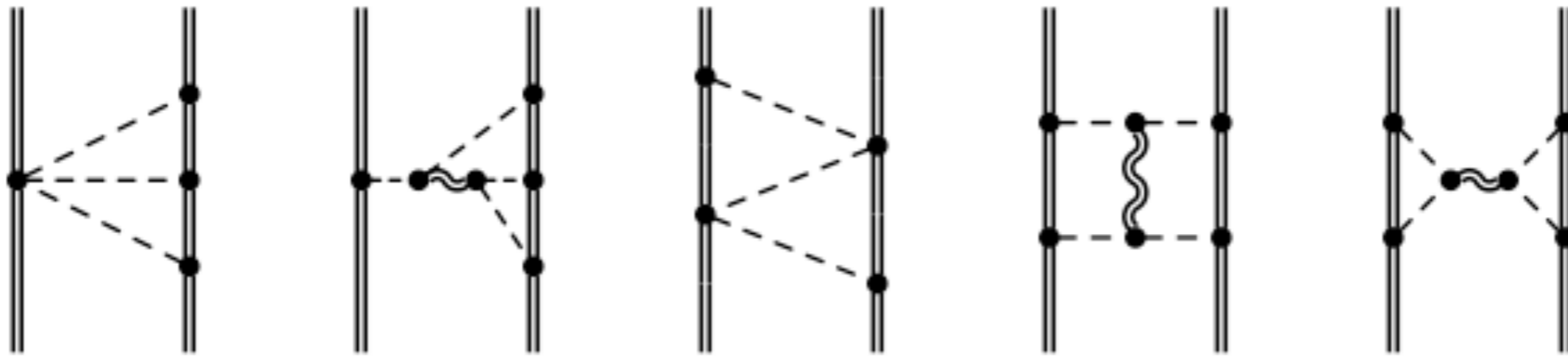


$$L_{EIH} = \frac{1}{8} \sum_a m_a \vec{v}_a^4 + \frac{G_N m_1 m_2}{2r} [3(\vec{v}_1^2 + \vec{v}_2^2) - 7\vec{v}_1 \cdot \vec{v}_2 - (\vec{v}_1 \cdot \vec{n})(\vec{v}_1 \cdot \vec{n})]$$

$$- \frac{G_N^2 m_1 m_2}{2r^2}$$

2PN (1981-2002): Some of the diagrams are

(Gilmore+Ross, PRD 2008)



$$\begin{aligned}
 L_{2PN} = & \frac{m_1 \mathbf{v}_1^6}{16} \\
 & + \frac{Gm_1 m_2}{r} \left( \frac{7}{8} \mathbf{v}_1^4 - \frac{5}{4} \mathbf{v}_1^2 \mathbf{v}_1 \cdot \mathbf{v}_2 - \frac{3}{4} \mathbf{v}_1^2 \mathbf{n} \cdot \mathbf{v}_1 \mathbf{n} \cdot \mathbf{v}_2 + \frac{3}{16} \mathbf{v}_1^2 \mathbf{v}_2^2 + \frac{1}{8} (\mathbf{v}_1 \cdot \mathbf{v}_2)^2 \right. \\
 & \quad \left. - \frac{1}{8} \mathbf{v}_1^2 (\mathbf{n} \cdot \mathbf{v}_2)^2 + \frac{3}{4} \mathbf{n} \cdot \mathbf{v}_1 \mathbf{n} \cdot \mathbf{v}_2 \mathbf{v}_1 \cdot \mathbf{v}_2 + \frac{3}{16} (\mathbf{n} \cdot \mathbf{v}_1)^2 (\mathbf{n} \cdot \mathbf{v}_2)^2 \right) \\
 & + Gm_1 m_2 \left( \frac{1}{8} \mathbf{a}_1 \cdot \mathbf{n} \mathbf{v}_2^2 + \frac{3}{2} \mathbf{a}_1 \cdot \mathbf{v}_1 \mathbf{n} \cdot \mathbf{v}_2 - \frac{7}{4} \mathbf{a}_1 \cdot \mathbf{v}_2 \mathbf{n} \cdot \mathbf{v}_2 - \frac{1}{8} \mathbf{a}_1 \cdot \mathbf{n} (\mathbf{n} \cdot \mathbf{v}_2)^2 \right) \\
 & + Gm_1 m_2 r \left( \frac{15}{16} \mathbf{a}_1 \cdot \mathbf{a}_2 - \frac{1}{16} \mathbf{a}_1 \cdot \mathbf{n} \mathbf{a}_2 \cdot \mathbf{n} \right) \\
 & + \frac{G^2 m_1 m_2^2}{r^2} \left( \frac{7}{4} \mathbf{v}_1^2 + 2 \mathbf{v}_2^2 - \frac{7}{2} \mathbf{v}_1 \cdot \mathbf{v}_2 + \frac{1}{2} (\mathbf{n} \cdot \mathbf{v}_1)^2 \right) \\
 & + \frac{G^3 m_1 m_2^3}{2r^3} + \frac{3G^3 m_1^2 m_2^2}{2r^3} + (1 \leftrightarrow 2),
 \end{aligned}$$

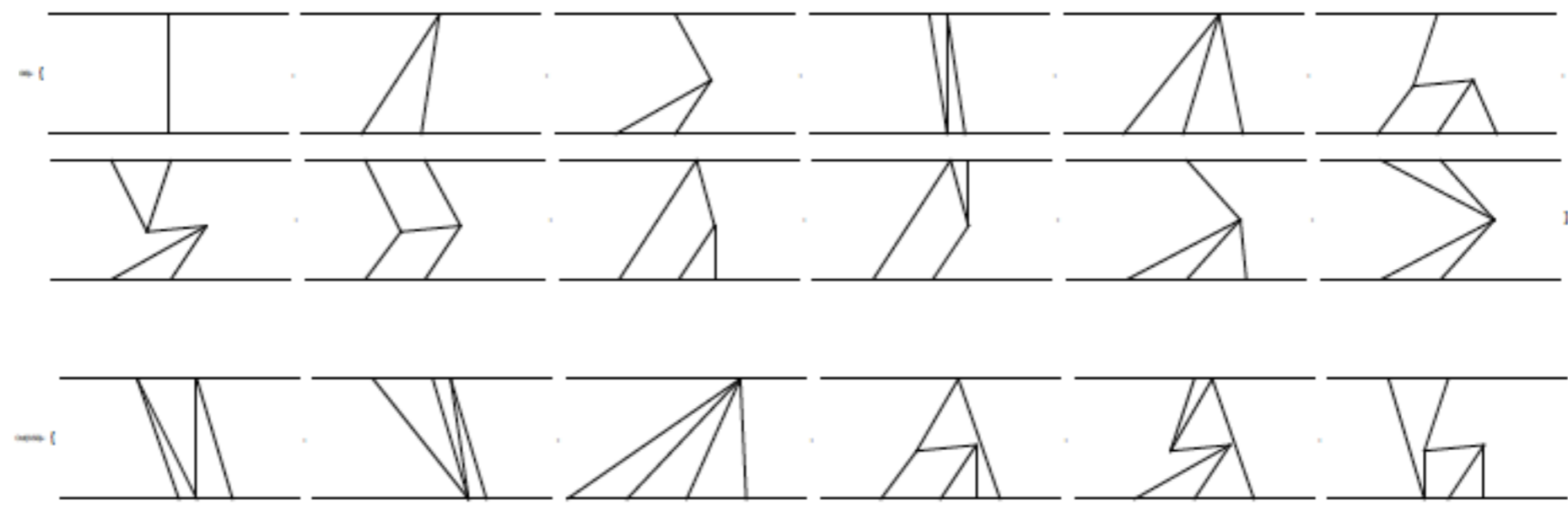
reducible to one-loop integrals via IBP:

$$\int \frac{d^{d-1} \mathbf{k}}{(2\pi)^{d-1}} \frac{1}{[(\mathbf{k} + \mathbf{p})^2]^\alpha [\mathbf{k}^2]^\beta}$$

(simplification of PT via field redefs: B. Kol+M. Smolkin, 2007-2008.)

**3PN (1998-2003):** Recently computed by Sturani+Foffa (2011). Computer generated Feynman diagrams plus table of standard Feynman integrals.

relevant topologies:



	0PN	1PN	2PN	3PN	4PN
$G$	1				
$G^2$		1	1		
$G^3$			5	4	
$G^4$				8	21
$G^5$					50

# topologies vs. PN order

	$v^0$	$v^2$	$v^4$	$v^6$
$G$	1	1	1	
$G^2$	1	8	7	7
$G^3$	5	48	159	...
$G^4$	8	299	...	
$G^4$	50	...		

# of diagrams/topology/ fixed PN order.

Partial progress in EFT computation of 4PN potentials has also been made. See Sturani + Foffa, PRD 2013.

## Inclusion of BH spin into the EFT: (R. Porto, PRD 2007)

“Hyperfine” (Spin-spin) interactions: (Porto+Rothstein, PRL 2008)

$$\begin{aligned}
 V_{3PN}^{ss} = & -\frac{G_N}{2r^3} \left[ \vec{S}_1 \cdot \vec{S}_2 \left( \frac{3}{2} \vec{v}_1 \cdot \vec{v}_2 - 3\vec{v}_1 \cdot \vec{n} \vec{v}_2 \cdot \vec{n} - (\vec{v}_1^2 + \vec{v}_2^2) \right) - \vec{S}_1 \cdot \vec{v}_1 \vec{S}_2 \cdot \vec{v}_2 - \frac{3}{2} \vec{S}_1 \cdot \vec{v}_2 \vec{S}_2 \cdot \vec{v}_1 + \vec{S}_1 \cdot \vec{v}_2 \vec{S}_2 \cdot \vec{v}_2 \right. \\
 & + \vec{S}_2 \cdot \vec{v}_1 \vec{S}_1 \cdot \vec{v}_1 + 3\vec{S}_1 \cdot \vec{n} \vec{S}_2 \cdot \vec{n} (\vec{v}_1 \cdot \vec{v}_2 + 5\vec{v}_1 \cdot \vec{n} \vec{v}_2 \cdot \vec{n}) - 3\vec{S}_1 \cdot \vec{v}_1 \vec{S}_2 \cdot \vec{n} \vec{v}_2 \cdot \vec{n} - 3\vec{S}_2 \cdot \vec{v}_2 \vec{S}_1 \cdot \vec{n} \vec{v}_1 \cdot \vec{n} \\
 & + 3(\vec{v}_2 \times \vec{S}_1) \cdot \vec{n} (\vec{v}_2 \times \vec{S}_2) \cdot \vec{n} + 3(\vec{v}_1 \times \vec{S}_1) \cdot \vec{n} (\vec{v}_1 \times \vec{S}_2) \cdot \vec{n} - \frac{3}{2} (\vec{v}_1 \times \vec{S}_1) \cdot \vec{n} (\vec{v}_2 \times \vec{S}_2) \cdot \vec{n} \\
 & \left. - 6(\vec{v}_1 \times \vec{S}_2) \cdot \vec{n} (\vec{v}_2 \times \vec{S}_1) \cdot \vec{n} \right] + \frac{3G_N^2(m_1 + m_2)}{r^4} (\vec{S}_1 \cdot \vec{S}_2 - 3\vec{S}_1 \cdot \vec{n} \vec{S}_2 \cdot \vec{n}),
 \end{aligned}$$

$\vec{S}^2$  – orbit couplings: (Porto+Rothstein, PRD 2008)

$$\begin{aligned}
 & = C_{ES^2}^{(1)} \frac{G_N m_2}{2m_1 r^3} [S_1^{j0} S_1^{i0} (3n^i n^j - \delta^{ij}) - 2S_1^{k0} ((\mathbf{v}_1 \times \mathbf{S}_1)^k - 3(\mathbf{n} \cdot \mathbf{v}_1)(\mathbf{n} \times \mathbf{S}_1)^k)] \\
 & + C_{ES^2}^{(1)} \frac{G_N m_2}{2m_1 r^3} \left[ \mathbf{S}_1^2 \left( 6(\mathbf{n} \cdot \mathbf{v}_1)^2 - \frac{15}{2} \mathbf{n} \cdot \mathbf{v}_1 \mathbf{n} \cdot \mathbf{v}_2 + \frac{13}{2} \mathbf{v}_1 \cdot \mathbf{v}_2 - \frac{3}{2} \mathbf{v}_2^2 - \frac{7}{2} \mathbf{v}_1^2 \right) \right. \\
 & + (\mathbf{S}_1 \cdot \mathbf{n})^2 \left( \frac{9}{2} (\mathbf{v}_1^2 + \mathbf{v}_2^2) - \frac{21}{2} \mathbf{v}_1 \cdot \mathbf{v}_2 - \frac{15}{2} \mathbf{n} \cdot \mathbf{v}_1 \mathbf{n} \cdot \mathbf{v}_2 \right) + 2\mathbf{v}_1 \cdot \mathbf{S}_1 \mathbf{v}_1 \cdot \mathbf{S}_1 \\
 & \left. - 3\mathbf{v}_1 \cdot \mathbf{S}_1 \mathbf{v}_2 \cdot \mathbf{S}_1 - 6\mathbf{n} \cdot \mathbf{v}_1 \mathbf{n} \cdot \mathbf{S}_1 \mathbf{v}_1 \cdot \mathbf{S}_1 + 9\mathbf{n} \cdot \mathbf{v}_2 \mathbf{n} \cdot \mathbf{S}_1 \mathbf{v}_1 \cdot \mathbf{S}_1 + 3\mathbf{n} \cdot \mathbf{v}_1 \mathbf{n} \cdot \mathbf{S}_1 \mathbf{v}_2 \cdot \mathbf{S}_1 \right] \\
 & - C_{ES^2}^{(1)} \frac{m_2 G_N}{2m_1 r^3} (\mathbf{S}_1^2 - 3(\mathbf{S}_1 \cdot \mathbf{n})^2) + C_{ES^2}^{(1)} \frac{m_2 G_N^2}{2r^4} \left( 1 + \frac{4m_2}{m_1} \right) (\mathbf{S}_1^2 - 3(\mathbf{S}_1 \cdot \mathbf{n})^2) \\
 & - \frac{G_N^2 m_2}{r^4} (\mathbf{S}_1 \cdot \mathbf{n})^2 + (\tilde{\mathbf{a}}_{1(1)}^{so})^l S_1^{0l} + \mathbf{v}_1 \times \mathbf{S}_1 \cdot \tilde{\mathbf{a}}_{1(1)}^{so} + 1 \leftrightarrow 2.
 \end{aligned}$$

= I for BH

# One graviton sector: radiation couplings (W.G.+A. Ross, PRD 2010)

Integrating out potential modes gives the couplings of 2-body system to radiation:

$$T^{\mu\nu} =$$

$v^0$   $\bar{h}_{\mu\nu}$   $+$   $v^2$   $\bar{h}_{\mu\nu}$   
 $+$   $\bar{h}_{\mu\nu}$   $+$   
 $+$   $\dots$   $\bar{h}_{\mu\nu}$

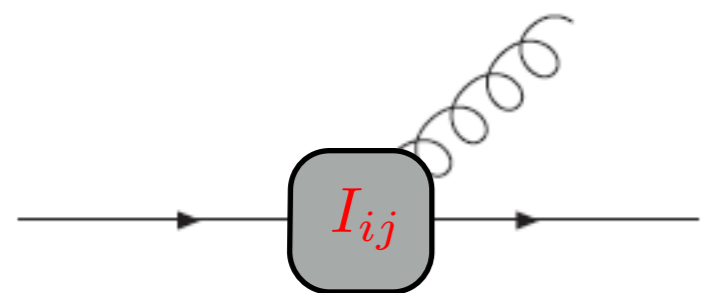
(1st graph=LO. Last three graphs are NLO).

The resulting action consists of a set of multipole moments coupled to the worldline of composite object. In the CM frame,

$$\Gamma[\bar{h}] = \frac{1}{2m_{Pl}} \int dx^0 \left[ I_E^{ij}(x^0) R_{0i0j} + \frac{4}{3} I_B^{i,jk}(x^0) R_{0jik} + \frac{1}{3} I_E^{ijk}(x^0) \nabla_k R_{0i0j} + \dots \right]$$

$\ell = 2_E$        $\ell = 2_B$        $\ell = 3_E$

For example, the quadrupole moment to NLO (Will+Wagoner, 1970's)



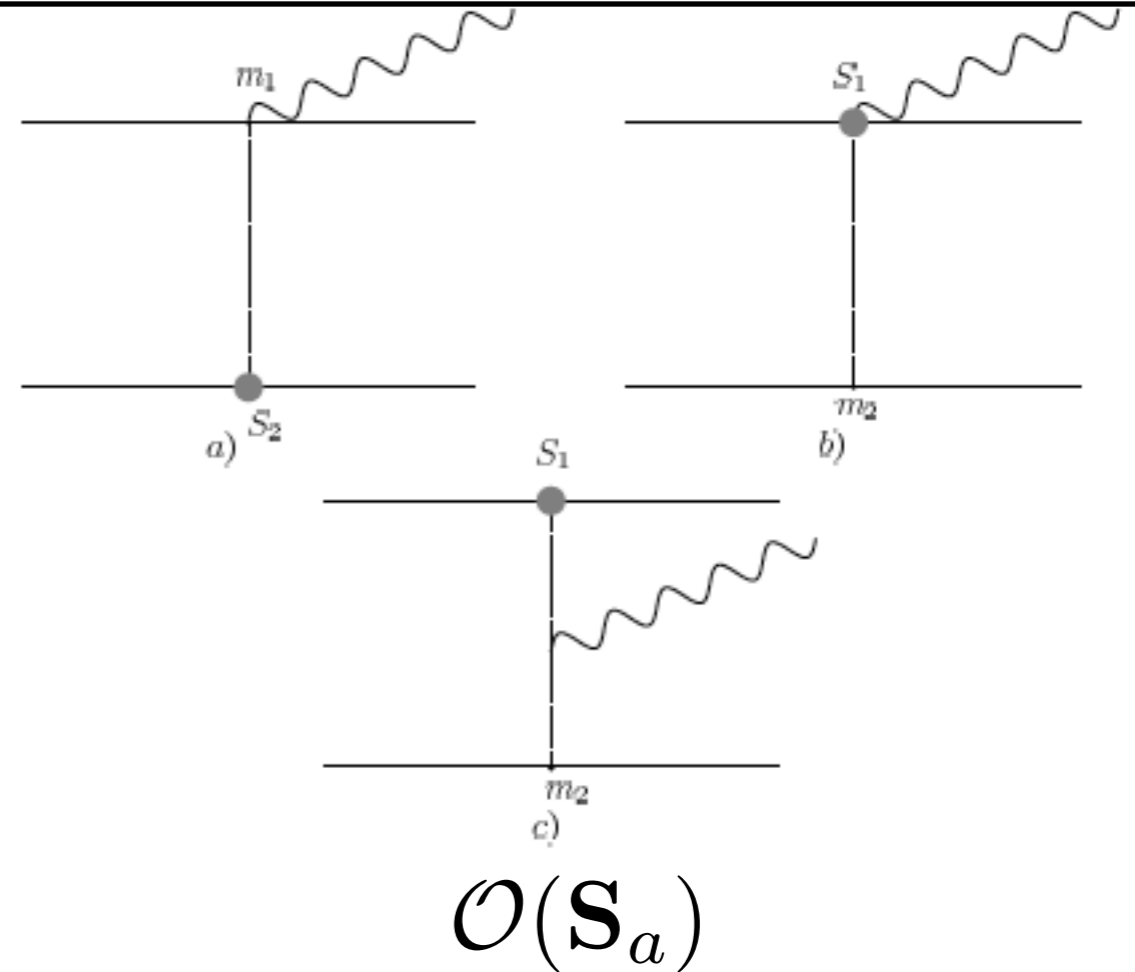
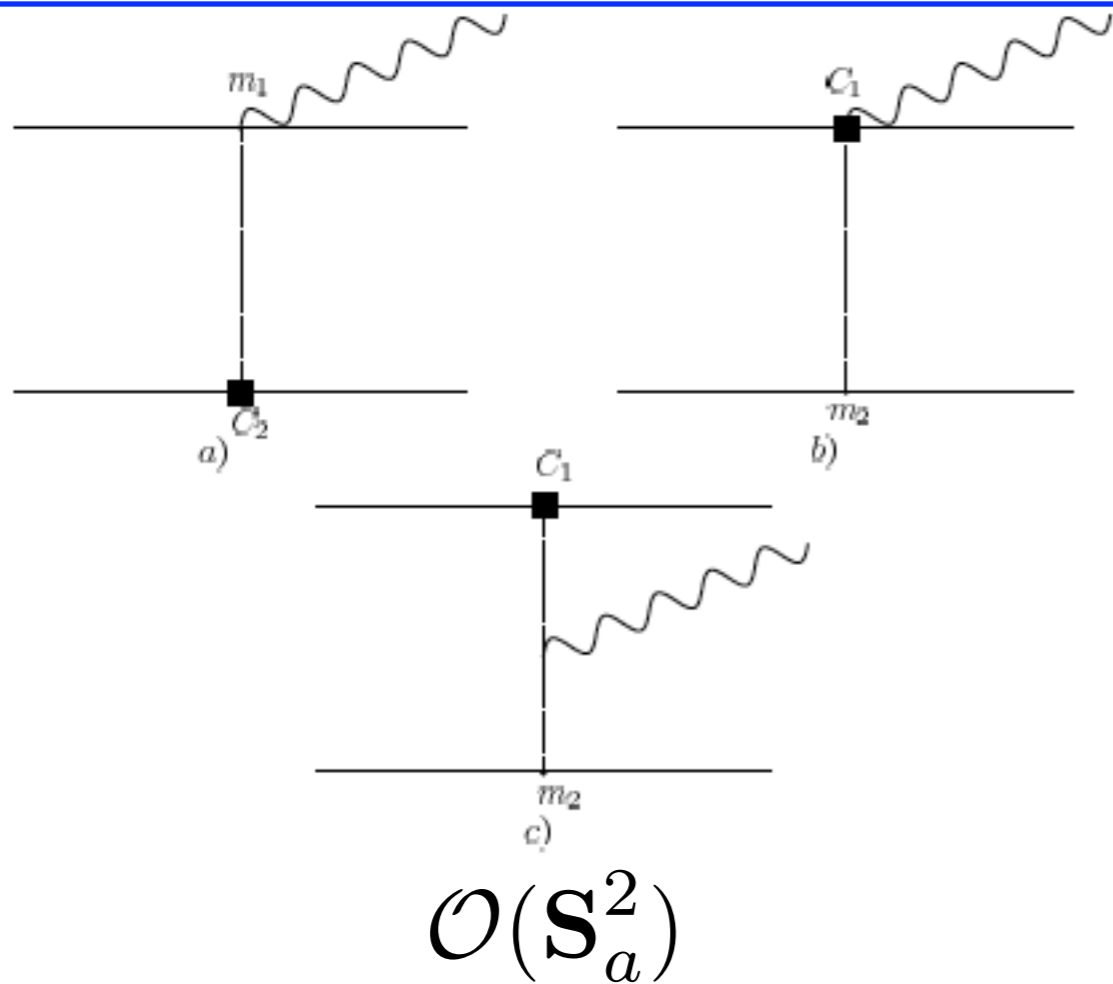
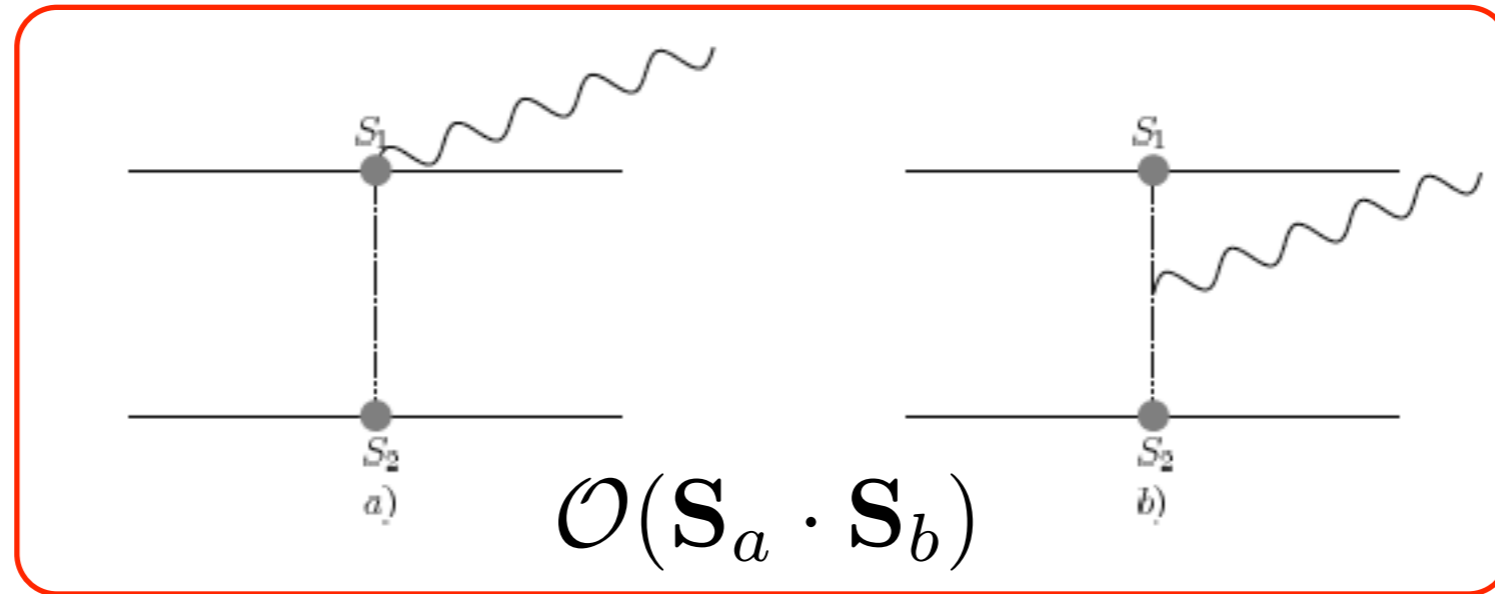
The diagram shows a grey rounded rectangle labeled  $I_{ij}$  with an arrow pointing to the right. A wavy line representing a gravitational wave is emitted from the top of the rectangle.

$$= \int d^3\mathbf{x} \left[ T^{00} + T^{aa} + \frac{11}{42} \mathbf{x}^2 \ddot{T}^{00} - \frac{4}{3} \dot{T}^{0k} x^k \right] [x^i x^j]^{TF} + \mathcal{O}(v^4)$$

$$= \sum_a m_a \mathbf{x}_a^i \mathbf{x}_a^j \left[ 1 + \frac{3}{2} \mathbf{v}_a^2 - \sum_b \frac{G_N m_b}{|\mathbf{x}_a - \mathbf{x}_b|} \right] + \frac{11}{42} \sum_a m_a \frac{d^2}{dt^2} (\mathbf{x}_a^2 \mathbf{x}_a^i \mathbf{x}_a^j)$$

$$- \frac{4}{3} \sum_a m_a \frac{d}{dt} (\mathbf{x}_a \cdot \mathbf{v}_a \mathbf{x}_a^i \mathbf{x}_a^j) - \text{traces} + \mathcal{O}(v^4)$$

This formalism has been used recently to compute spin-induced moments at 3PN order (Porto+Ross+Rothstein 2011)





# EFTIII: Radiation

(Double expansion:  $\eta_2 = r/\lambda \sim v$   
 $\eta_3 = r/r_g \sim v^3$  )

(WG+Ross, PRD 2010)

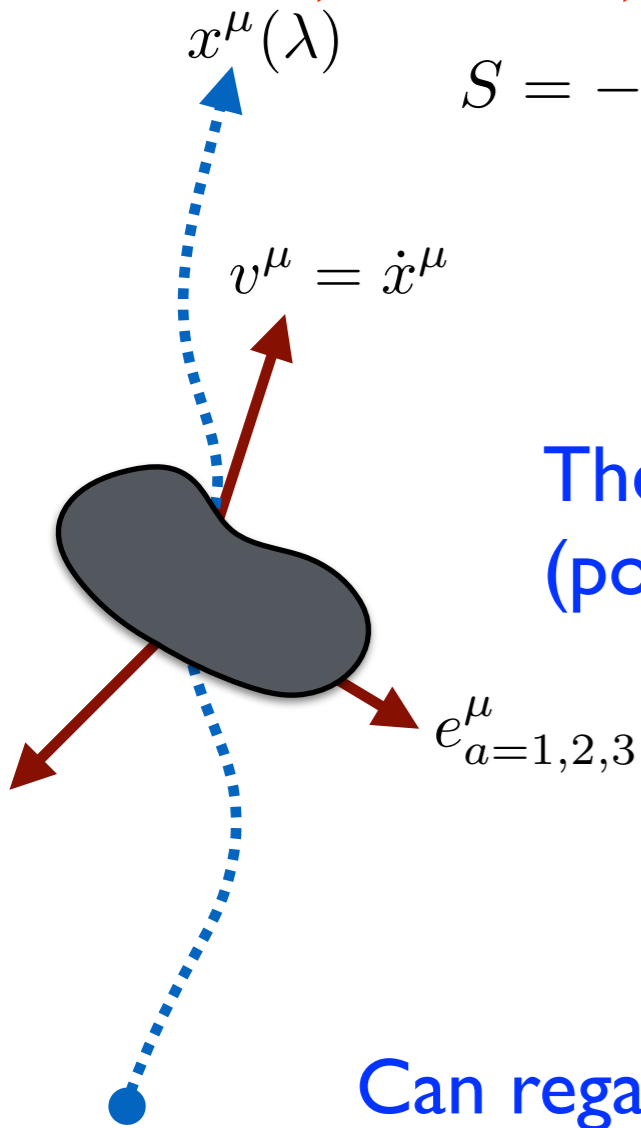
This is a field theory of radiation coupled to a point object with multipole moments. Most general diff. invariant action (**Elegant coset formulation:**

**S. Endlich, R. Penco, ..., 2014**)

$$S = - \int d\tau(\lambda) m(\lambda) - \int dx^\mu L_{ab}(\lambda) \omega_\mu^{ab}(x(\tau)) + \frac{1}{2} \int d\tau(\lambda) I_{ab}(\lambda) E^{ab}(x(\tau)) \\ - \frac{2}{3} \int d\tau J_{ab}(\lambda) B^{ab}(x) + \frac{1}{6} \int d\tau I_{abc}(\lambda) \nabla^c E^{ab}(x) + \dots$$

The time evolution of the moments arises from short dist. (potentials) as well as radiative corrections (radiation reaction).

Can regard the moments as time-dependent **Wilson coefficients** (coupling constants). Radiative corrections in the EFT will generate **RG flows** for them.



Can use this theory to compute observables at infinity, even if the short distance time evolution of the moments is not known. For example, the graviton emission amplitude involving the 1st three moments:

$$\begin{aligned}
 i\mathcal{A}_h(\mathbf{k}) &= \begin{array}{c} I^{ij} \\ \text{---} \\ \bullet \\ \text{---} \\ \text{wavy line} \end{array} + \begin{array}{c} J^{ij} \\ \text{---} \\ \bullet \\ \text{---} \\ \text{wavy line} \end{array} + \begin{array}{c} I^{ijk} \\ \text{---} \\ \bullet \\ \text{---} \\ \text{wavy line} \end{array} + \dots \\
 &= \frac{i}{4m_{Pl}} \epsilon_{ij}^*(\mathbf{k}, h) \left[ \mathbf{k}^2 I^{ij}(k) + \frac{4}{3} |\mathbf{k}| k^l \epsilon^{ikl} J^{jk}(k) - \frac{i}{3} \mathbf{k}^2 k^l I^{ijl}(k) + \dots \right]
 \end{aligned}$$

Determines the time averaged energy loss rate of the composite system:

$$\dot{P}^0 = \frac{G_N}{5} \left\langle \left( \frac{d^3}{dt^3} I^{ij}(t) \right)^2 \right\rangle + \frac{16G_N}{45} \left\langle \left( \frac{d^3}{dt^3} J^{ij}(t) \right)^2 \right\rangle + \frac{G_N}{189} \left\langle \left( \frac{d^4}{dt^4} I^{ijk}(t) \right)^2 \right\rangle + \dots$$

(To do calculations like these, need the sum over graviton polarizations

$$\sum_h \epsilon_{ij}(\mathbf{k}, h) \epsilon_{rs}^*(\mathbf{k}, h) = \frac{1}{2} \left[ \delta_{ir} \delta_{js} + \delta_{is} \delta_{jr} - \delta_{ij} \delta_{rs} + \frac{1}{\mathbf{k}^2} (\delta_{ij} \mathbf{k}_r \mathbf{k}_s + \delta_{rs} \mathbf{k}_i \mathbf{k}_j) \right. \\ \left. - \frac{1}{\mathbf{k}^2} (\delta_{ir} \mathbf{k}_j \mathbf{k}_s + \delta_{is} \mathbf{k}_j \mathbf{k}_r + \delta_{jr} \mathbf{k}_i \mathbf{k}_s + \delta_{js} \mathbf{k}_i \mathbf{k}_r) + \frac{1}{\mathbf{k}^4} \mathbf{k}_i \mathbf{k}_j \mathbf{k}_r \mathbf{k}_s \right]$$

see eg Weinberg's GR textbook.

# UV and IR divergences in radiation

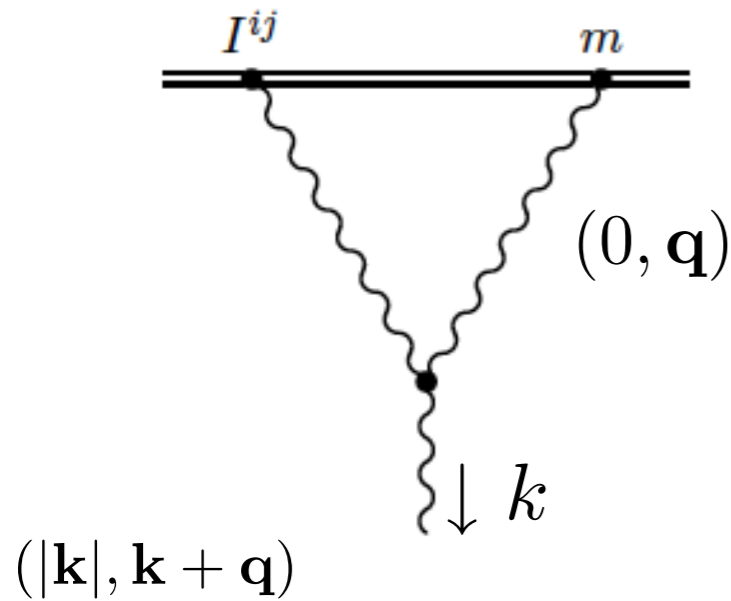
Focus on the  $\ell = 2$  channel. The amplitude to second order is

$$i\mathcal{A}(k) =$$

The diagram illustrates the amplitude  $i\mathcal{A}(k)$  as a sum of Feynman diagrams. Each diagram shows a source (represented by a horizontal line) with multipole moments  $I^{ij}$  and  $m$ . The source emits a graviton with momentum  $k$  (represented by a wavy line). The diagrams are summed together with red plus signs, indicating a series expansion. The first diagram shows a single vertex  $I^{ij}$  emitting a graviton with momentum  $k$ . The second diagram shows a vertex  $I^{ij}$  and a vertex  $m$  connected by a graviton line, with a graviton line from  $I^{ij}$  to the external  $k$ . The third diagram shows a vertex  $I^{ij}$  and two vertices  $m$  connected by two graviton lines, with a graviton line from  $I^{ij}$  to the external  $k$ . The fourth diagram shows a vertex  $I^{ij}$  and two vertices  $m$  connected by two graviton lines, with a graviton line from the second  $m$  vertex to the external  $k$ . The fifth diagram shows a vertex  $I^{ij}$  and two vertices  $m$  connected by two graviton lines, with a graviton line from the first  $m$  vertex to the external  $k$ . The series continues with an ellipsis.

Non-linear interaction of emitted gravitons with multipole moments introduces both UV and IR divergences.

Leading IR divergence: The order  $\eta_3 \sim v^3$  correction to the amplitude:



Can be reduced to scalar Feynman integrals of the form

$$I_n(|\mathbf{k}|) = \int \frac{d^{d-1} \mathbf{q}}{(2\pi)^{d-1}} \frac{(\mathbf{q}^2)^n}{\mathbf{k}^2 - (\mathbf{k} + \mathbf{q})^2 + i\epsilon}$$

$$(n \geq -1)$$

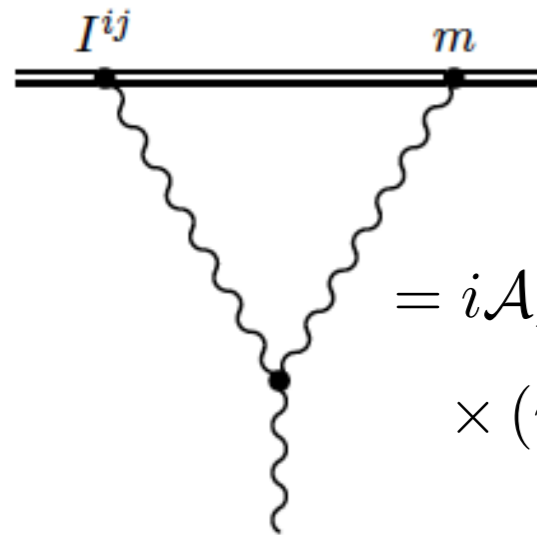
Note that for  $n = -1$  this has an infrared divergence.

As  $\mathbf{q} \rightarrow 0$  ( $d = 4 - 2\epsilon$ )

$$I_{-1}(|\mathbf{k}|) = \int \frac{d^{d-1} \mathbf{q}}{(2\pi)^{d-1}} \frac{1}{\mathbf{q}^2} \frac{1}{\mathbf{k}^2 - (\mathbf{k} + \mathbf{q})^2 + i\epsilon} \sim \int \frac{d^3 \mathbf{q}}{(2\pi)^3} \frac{1}{\mathbf{q}^2 (\mathbf{k} \cdot \mathbf{q})} \sim \frac{1}{\epsilon_{IR}}$$

Physically, this is the familiar “Coulomb” singularity: nearly on-shell graviton interacts with the long range  $1/r$  potential of the composite object.

The complete result is



$$= i\mathcal{A}_{LO} \times (iG_N m |\mathbf{k}|) \left[ -\frac{(\mathbf{k}^2 + i\epsilon)}{\pi\mu^2} e^{\gamma_E} \right]^{(d-4)/2} \times \left[ \frac{2}{(d-4)_{IR}} - \frac{11}{6} + (d-4) \left( \frac{\pi^2}{8} + \frac{203}{72} \right) \right]$$

Note that to order  $G_N m |\mathbf{k}| \sim v^3$ , the IR singularities drop from  $|\mathcal{A}|^2$

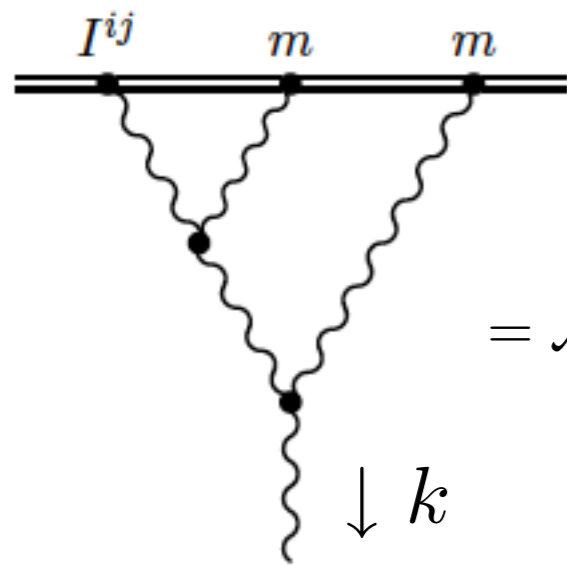
$$\left| \frac{\mathcal{A}}{\mathcal{A}_{LO}} \right|^2 = 1 + 2G_N m |\mathbf{k}| + \mathcal{O}(1/\epsilon_{IR}^2)$$

The “Coulomb tail” is responsible for non-analytic corrections to the radiated power in gravitons. Eg,

$$P_{v^3} = P_{LO} \times (4\pi v^3) \qquad P_{v^5} = P_{LO} \times \left( -\frac{8191}{672} \pi v^5 \right)$$

## Subleading IR divergences:

The following order  $\eta_3^2 \sim v^6$  diagram is also IR divergent by power counting



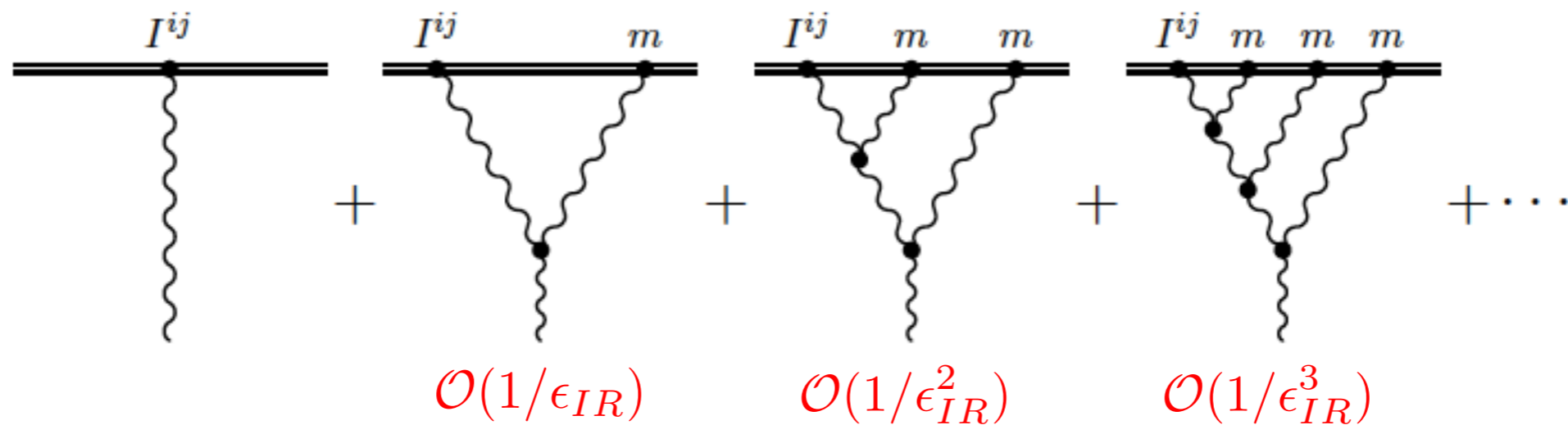
$$= \mathcal{A}_{LO} (G_N m |\mathbf{k}|)^2 \left[ -\frac{(\mathbf{k}^2 + i\epsilon)}{\pi\mu^2} e^{\gamma_E} \right]^{(d-4)} \times \left[ -\frac{2}{(d-4)_{IR}^2} + \frac{11}{3} \frac{1}{(d-4)_{IR}} + \dots \right]$$

but one can check that all IR divergences cancel out of physical quantities, up to higher order terms in perturbation theory. E.g:

$$\left| \mathcal{A}_{\mathcal{O}(\eta_3^2)} \right|^2 = \left| \text{Diagram} \right|^2 + 2 \operatorname{Re} \left( \text{Diagram} \right)$$

is independent of  $1/\epsilon_{IR}$

We also showed that the leading  $1/\epsilon_{IR}$  poles at each order, from the diagrams



sum up to a complex phase in the emission amplitude,

$$\mathcal{A} = \exp \left[ \frac{2iG_N m \omega}{(d-4)_{IR}} \right] \mathcal{A}_{\text{finite}} \rightarrow |\mathcal{A}|^2 = \text{IR finite}$$

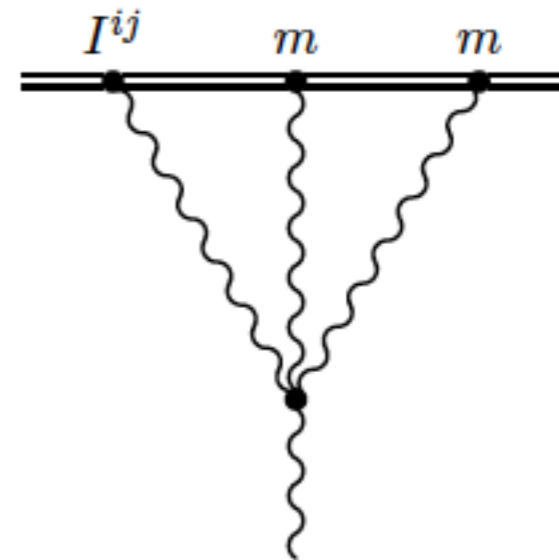
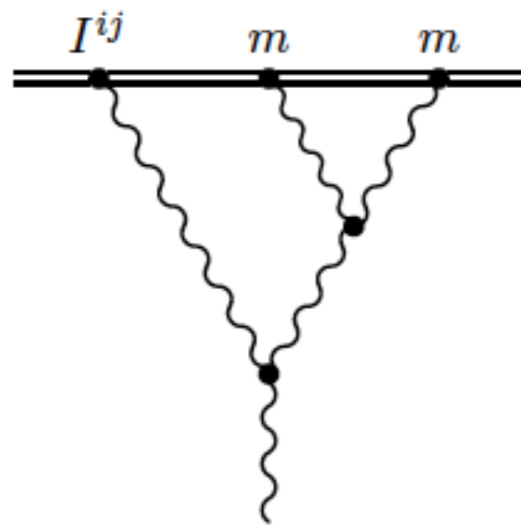
so poles drop out of physical predictions.

The handling of IR divergences in the waveform  $h_{ij}^{TT}(t, \mathbf{x} \rightarrow \infty)$  has been recently addressed. (Porto, Ross, Rothstein, arXiv/2003.2962).



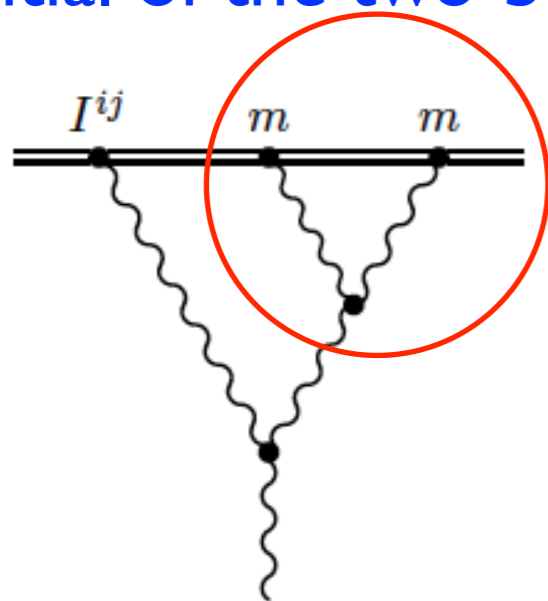
# Leading UV divergences

The following graphs at order  $\eta_3^2 \sim v^6$



are logarithmically UV divergent.

This reflects the interaction of nearly on-shell outgoing graviton with the  $1/r^2$  potential of the two-body system. Eg.



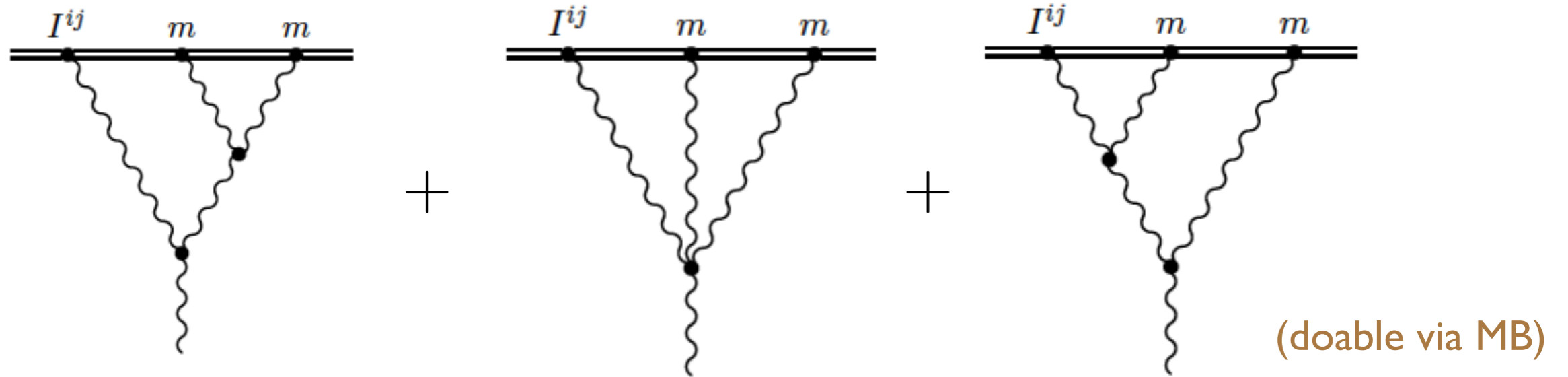
$$\sim \frac{1}{|\mathbf{q}|}$$



$$\int \frac{d^d \mathbf{q}}{(2\pi)^d} \frac{1}{|\mathbf{q}|} \frac{1}{\mathbf{k}^2 - (\mathbf{k} + \mathbf{q})^2 + i\epsilon}$$

$$\sim \int \frac{d^3 \mathbf{q}}{(2\pi)^3} \frac{1}{|\mathbf{q}|^3} \sim \frac{1}{\epsilon_{UV}}$$

The full result at second order in the expansion is then



$$\frac{\mathcal{A}_{\eta^2}}{\mathcal{A}_{\eta^0}} = (G_N m |\mathbf{k}|)^2 \left[ -\frac{(\mathbf{k}^2 + i\epsilon)}{\pi\mu^2} e^{\gamma_E} \right]^{-2\epsilon} \times \left[ -\frac{1}{2\epsilon_{IR}^2} - \frac{11}{6} \frac{1}{\epsilon_{IR}} + \frac{107}{210} \frac{1}{\epsilon_{UV}} - \frac{7\pi^2}{12} - \frac{1777}{14700} \right].$$

# RG flows

UV divergences correspond to singularities in the multipole expansion, first at  $\eta_3^2 \sim v^6$ . In the EFT, these divergences are absorbed into the Wilson coefficients, i.e, **renormalization of the multipole moments**

$$\mu \frac{d}{d\mu} I_{ij}^R(\omega, \mu) = -\frac{214}{105} (G_N m \omega)^2 I_{ij}^R(\omega, \mu),$$



$$I_{ij}(\omega, \mu) = \left[ \frac{\mu}{\mu_0} \right]^{-\frac{214}{105} (G_N m \omega)^2} I_{ij}(\omega, \mu_0).$$

This can be used to predict the pattern of logs  $\sim \eta^{2n} \log^n \eta$  in quadrupole radiation:

$$\left| \frac{\mathcal{A}(\omega)}{\mathcal{A}_{\eta^0}(\omega, \mu_0)} \right|_{\text{leading log}}^2 = 1 - \frac{428}{105} (G_N m \omega)^2 \ln \frac{\omega}{\mu_0} + \frac{91592}{11025} (G_N m \omega)^4 \ln^2 \frac{\omega}{\mu_0} - \frac{39201376}{3472875} (G_N m \omega)^6 \ln^3 \frac{\omega}{\mu_0} + \dots$$

For circular orbits, our prediction is

$$\frac{\dot{E}_{LL}}{\dot{E}_{LO}} = v^{-\frac{1712}{105}} v^6 = 1 - \frac{1712}{105} v^6 \ln v + \frac{1465472}{11025} v^{12} \ln^2 v - \frac{2508888064}{3472875} v^{18} \ln^3 v + \dots$$

This was confirmed recently by BH perturbation theory (R. Fujita, arXiv:1211.5535)

$$\begin{aligned} \frac{dE}{dt} = & \left( \frac{dE}{dt} \right)_N \left[ 1 - \frac{1247}{336} v^2 + 4\pi v^3 - \frac{44711}{9072} v^4 - \frac{8191}{672} \pi v^5 \right. \\ & + \left\{ \frac{6643739519}{69854400} - \frac{1712}{105} \gamma - \frac{3424}{105} \ln(2) + \frac{16}{3} \pi^2 - \frac{1712}{105} \ln(v) \right\} v^6 - \frac{16285}{504} \pi v^7 \\ & + \left\{ -\frac{323105549467}{3178375200} + \frac{232597}{4410} \gamma + \frac{39931}{294} \ln(2) - \frac{1369}{126} \pi^2 - \frac{47385}{1568} \ln(3) \right. \\ & \quad \left. + \frac{232597}{4410} \ln(v) \right\} v^8 \\ & + \left\{ \frac{265978667519}{745113600} \pi - \frac{13696}{105} \ln(2) \pi - \frac{6848}{105} \pi \gamma - \frac{6848}{105} \pi \ln(v) \right\} v^9 \\ & + \left\{ -\frac{2500861660823683}{2831932303200} + \frac{916628467}{7858620} \gamma - \frac{83217611}{1122660} \ln(2) - \frac{424223}{6804} \pi^2 \right. \\ & \quad \left. + \frac{47385}{196} \ln(3) + \frac{916628467}{7858620} \ln(v) \right\} v^{10} \\ & + \left\{ \frac{177293}{1176} \pi \gamma + \frac{8521283}{17640} \ln(2) \pi + \frac{8399309750401}{101708006400} \pi - \frac{142155}{784} \pi \ln(3) + \frac{177293}{1176} \pi \ln(v) \right\} v^{11} \\ & + \left\{ -\frac{256}{45} \pi^4 - \frac{37744140625}{260941824} \ln(5) + \frac{2067586193789233570693}{602387400044430000} \right. \\ & \quad - \frac{246137536815857}{157329572400} \gamma - \frac{27392}{105} \zeta(3) - \frac{437114506833}{789268480} \ln(3) \\ & \quad - \frac{271272899815409}{157329572400} \ln(2) + \frac{5861888}{11025} \ln(2) \gamma - \frac{54784}{315} \ln(2) \pi^2 \\ & \quad + \frac{3803225263}{10478160} \pi^2 - \frac{27392}{315} \pi^2 \gamma + \frac{5861888}{11025} \ln(2)^2 + \frac{1465472}{11025} \gamma^2 \\ & \quad + \left( \frac{2930944}{11025} \gamma - \frac{27392}{315} \pi^2 - \frac{246137536815857}{157329572400} + \frac{5861888}{11025} \ln(2) \right) \ln(v) \\ & \quad \left. + \frac{1465472}{11025} \ln(v)^2 \right\} v^{12} + \dots - 722.42394673001478 \ln(v)^3 v^{18} + \dots \end{aligned} \approx \frac{2508888064}{3472875}$$

This result can be extended to the  $\ell > 2$  moments, using the methods developed in Ross, arXiv:1202.4750. The general pattern of logs is

$$|\mathcal{A}_\ell(\omega)|^2 \sim S(\omega) \sum_{n=1}^{\infty} \eta^{2n} L \left[ \beta_{2n}^{(\ell)} + \mathcal{O}(\eta^2 L) + \mathcal{O}(\eta^2 L)^2 + \mathcal{O}(\eta^2 L)^3 + \dots \right],$$

Sommerfeld

factor

$$S(\omega) = \frac{4\pi G_N m \omega}{1 - \exp(-4\pi G_N m \omega)}.$$

Fixes the series of logs

Maybe useful for the construction of phenomenological templates...

Other recent results in the radiation sector:

Radiation reaction at 3.5PN (1993-1995) (Galley+Leibovich, 2012). 4 PN in progress (2011 Wang et al).

3PN Flux and 2.5PN waveform for spin-induced moments (Porto, Ross, Rothstein, 2010,2012).

Hereditary terms in radiation reaction at 4PN (Foffa+Sturani, 2011) (Blanchet et al 2010)